LASCO AND EIT OBSERVATIONS OF THE DYNAMIC CORONA

K. P. DERE AND G. E. BRUECKNER
Naval Research Laboratory, Code 7660
Washington DC 20375

1. Introduction

The combined operations of the Large Angle Spectrometric Coronagraph (LASCO) and the Extreme Ultraviolet Imaging Telescope (EIT) on the Solar and Heliospheric Observatory (SOHO), launched in December 1995, have provided an unprecedented opportunity for observing essentially all coronal phenomena that are not hidden behind the disk of the Sun. Consequently, observations with these instrument are providing information on coronal mass ejections (CMEs) from their initiation through their development over 30 $R_\odot$. They reveal a coronal that never reaches a steady state. The corona is the site of continuous, time-dependent outflows, both within the coronal holes and the high speed streams and in the streamer belts and their mid-latitude sources. The spatial scales of these outflows range from 10s of arc-seconds through about a solar radius in large CMEs.

A detailed description of the EIT and LASCO instruments is provided by Delaboudiniere et al. (1995) and Brueckner et al. (1995). Briefly, the EIT consists of a Ritchey-Chretien telescope with EUV reflecting multilayer coatings, several filters and a CCD detector. Different multilayer coatings are placed on 4 quadrants of both the primary and secondary mirrors in order that any 1 of 4 wavelengths ranges can be observed at a given time, while providing a good registration of images obtained in the four wavelengths. The EIT observations that we will discuss were obtained with the 195 Å Fe XII channel. Fe XII is emitted most efficiently at temperatures near 1.5 x 10^6 K. The observed pattern of emission at 195Å is also affected by the presence of absorbing features. Absorption of coronal emissions is often noticed in all 3 of the coronal channels at locations of prominences and macrospicules, both seen in He II. The mechanism for this absorption is probably photo-ionization of He I and/or He II. This turns out to be a particularly useful feature since, in this case, it allows one to see both the prominence and coronal structures in the CME.

The LASCO instrument consists of an internally occulted coronagraph, C1, and 2 externally occulted coronagraphs, C2 and C3. The C1 coronagraph is able to observe the corona to within about 1.1 $R_\odot$ with a field of view that extends to about 3 $R_\odot$. Observations with C1 are made through a tunable, narrow-band Fabry-Perot filter. The field of view of C2 extends from about 1.5 $R_\odot$, the edge of the occulter, to 6 $R_\odot$. Similarly, the C3 coronagraph has a field of view from 4 to 30 $R_\odot$. The signal in C2 and C3 consists of broad-band visible photospheric light scattered primarily by electrons in the corona.

2. LASCO and EIT observations of the initiation of a CME

A key requirement for detecting the initiation of a CME is the ability to view the full disk of the Sun at a high cadence. This was not achieved with the EIT until a period near the end of December 1996 when a large fraction of the SOHO telemetry resources were devoted to EIT and LASCO. A combined observing program was run where the EIT obtained full disk images in Fe XII roughly every 12 minutes. LASCO obtained a C1 Fe XIV image every 24 minutes, a C2 image every 24 minutes and a C3 image every 50 minutes. EIT observations of the initiation of a CME on December 23, 1996 are shown in Figure 1, where running differences of the EIT 195Å images are shown.

The first evidence of the CME is the acceleration of a short (35 arc-sec.) segment of cool prominence material ('EP' in Fig. 1) at 2020 UT accompanied by a small brightening ('B') which

J. Andersen (ed.), Highlights of Astronomy, Volume 11B, 861–864.

https://doi.org/10.1017/S1539299600018955 Published online by Cambridge University Press

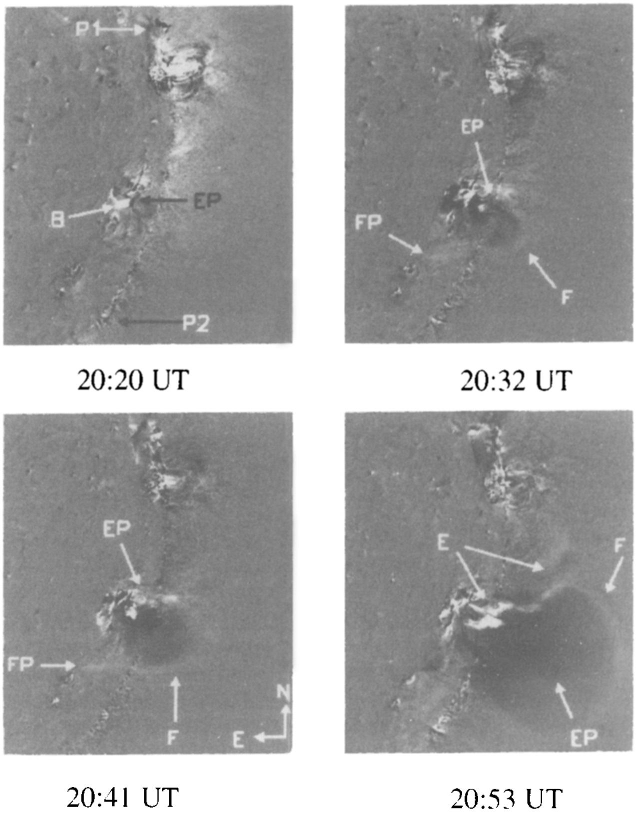

Figure 1. EIT running difference images of the initiation of a CME. The letters in the figures are used to indicate the following structures: EP, the eruptive prominence; B, the flare-like brightening; P1 and P2, prominences; F, the outer front of the CME; FP, the suspected footpoint of one side of the CME; E, a secondary set of ejecta. Solar north and east are as indicated in the images at 20:41 UT.

is probably associated with a small (B2) X-ray flare observed by GOES. The four images in Fig. 1 show the development of the CME which by 2053 exhibits all 3 components of a classical CME: the bright loop-like front ('F'), the eruptive prominence ('EP') and the dark void inside (Kahler, 1987). The CME continues to expand into the field of view of the LASCO where it reaches a velocity of about 400 km s^{-1}. In the C2 coronagraph, the streamer overlying the location of the CME brightened steadily in the hours before the CME occurred. Perhaps the most important thing demonstrated by these observations is that, while a CME clearly involves large scale structures such as seen in the brightening of the streamer, the CME did not actually occur until it was initiated by the ejection of a small section of prominence plasma.

At first glance, the December 23 CME would appear to be a fairly simple CME. However, there are a number of factors to note. First, the active region in which the CME was initiated had first appeared almost exactly 1 solar rotation previously but by December 23 it was rapidly decaying and could not be seen on the next rotation. Second, this CME seemed to be associated with considerable coronal activity along the same longitude. At 2053 UT, continued ejection of plasma ('E') is seen that appears to be connected with the active region to the north, which produced a small CME somewhat earlier. To the south, a small prominence was later ejected and was accompanied by the expansion of large coronal loops. In addition, the CME also appeared to be the origin of a faint coronal wave that emanated outward from the site of the CME at a velocity of about 80 km s^{-1}.

https://doi.org/10.1017/S1539299600018955 Published online by Cambridge University Press

Since this event, more striking examples of coronal waves have been observed. A more complete discussion can be found in Dere *et al.* (1997).

3. Earth directed CMEs

An important aspect of CMEs is that they often impact the Earth's magnetosphere and cause geomagnetic storms. One observational key is that Earth-directed (and anti-directed) CMEs appear as 'halos' about the occulting disk. The first halo event was observed with the SOLWIND experiment (Howard *et al.* 1982). A good example of a halo CME occurred on April 7, 1997. In this case, the event starts as a flare seen in the 195Å channel at 1400 UT. In the next immediate frame at 1412 UT, a bright wave has propagated a distance of about 5 arc-min., or a good portion of the solar disk. The flare occurred in the SE quadrant of the disk.

By 1459 UT, a CME is well apparent in the C2 image at about 3.5 $R_\odot$ with the brightest emission also in the SE quadrant. However, bright features are beginning to appear at locations all around the Sun and by 1521 UT it is clear that a 'halo' CME is in progress. The LASCO C2 image at 1521 in shown in Figure 2. One thing to be noted about this 'halo' CME is the considerable amount of structure present in the event. The April 7 CME did arrive at the Earth and resulted in an intense geomagnetic storm with a K_p index of 7.

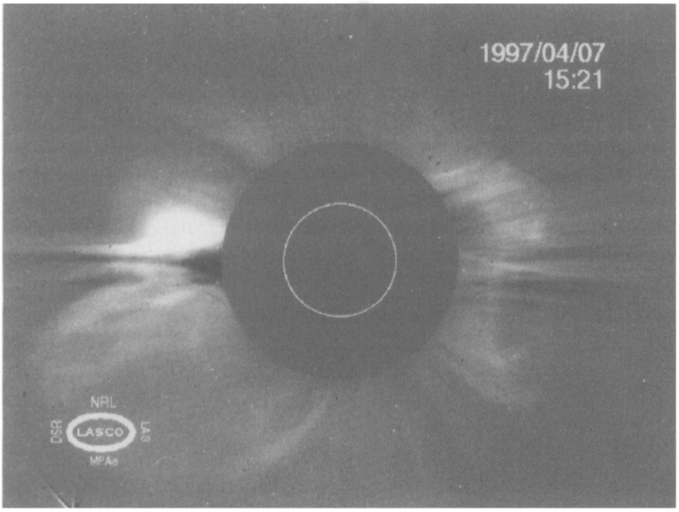

Figure 2. The LASCO C2 image of a 'halo' type CME. The white circle indicates the size and position of the solar disk.

4. The magnetic topology of CMEs

In the past, there have been numerous observations of CMEs. The nature of the mechanism that propels them into the heliosphere remains a central question. Their magnetic topology is directly related to this problem. Previous observations of CMEs that occur near the plane of the sky suggest that they are magnetic loops or arcades of loops. However, the halo CMEs indicate a real 3 dimensional character. The observations of the fine structure of the April 7 halo CME discussed above also suggests that the CME magnetic topology is complex. Theoretical models have often suggested the need for a helical flux geometry (Mouschovias and Poland 1978, Chen 1989, Low 1996, Wu *et al.* 1997).

The LASCO coronagraphs have now detected a considerable number of CMEs that appear to have a helical magnetic field structure. An example of one of these is shown in Figure 3 where running difference images from the C2 coronagraph are displayed. Not all CMEs observed by

https://doi.org/10.1017/S1539299600018955 Published online by Cambridge University Press

LASCO have the helical appearance but a significant fraction clearly indicate such structure. In these cases, the observations do indicate that the loop minor radius is smaller than the major radius but not to a large degree. These are not tightly coiled loops that when observed edge on would give the appearance of the loop-like structures commonly associated with CMEs.

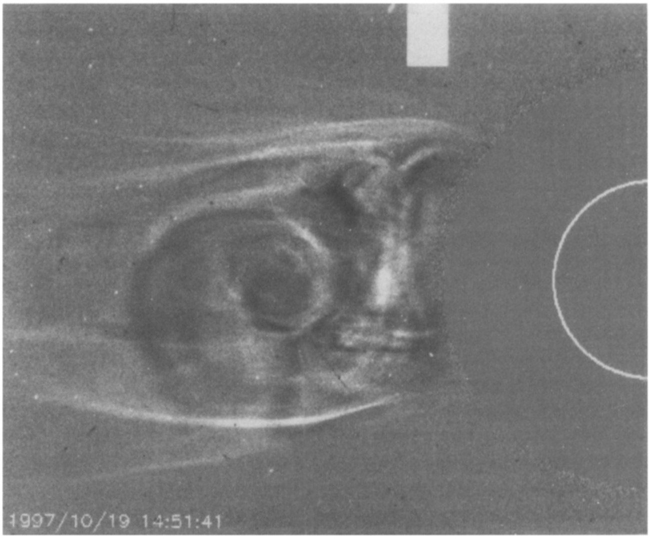

Figure 3. The LASCO C2 image of a CME with structure indicative of a helical magnetic field topology. The white circle indicates the size and position of the solar disk.

5. The dynamic corona

As noted in the introduction, the LASCO observations have demonstrated that the solar corona is in a highly dynamic state. This cannot be conveyed to the reader by any number of still frames. During the period 22-27 December, 1996, the LASCO coronagraphs operated at an enhanced telemetry rate so that it was able to obtain and downlink full-frame, full-resolution images with a 50 minute cadence for C3 and a 24 minute cadence for C2. These movies are available on the Web at the following URL:

http://lasco-www.nrl.navy.mil/public_movies.html

In addition to showing the continually varying outflows in the solar wind, the rapid temporal variations in the streamers and several CMEs, a sungrazing comet enters the field of view. In the background, the Milky Way is seen as it slowly passes through the C3 field of view. The movie is highly recommended.

This work was supported by the NASA.

References

Brueckner, G. E., et al., 1995, Solar Phys., **162**, 357
Chen, J.,1989, ApJ, **338**, 453
Delaboudiniere, J.-P. et al., 1995, Solar Phys., **162**,291
Dere, K. P. et al., 1997, Solar Phys., in press
Howard, R.A., Michels, D.J., Sheeley, Jr., N.R., Koomen, M.J., 1982, ApJL, **263**, L101
Kahler, S.,, 1987, in Proceedings of the Sixth International Solar Wind Conference, V. J. Pizzo, T. Holzer, and D. G. Sime (eds), NCAR TN-306, 215
Low, B. C., 1996, Solar Phys., **167**, 217
Mouschovias, T. C., Poland, A. I., 1978, ApJ, **220**, 675
Wu, S. T., Guo, W. P., Dryer, M., 1997, Solar Phys., **170**, 265.